Detrital Heavy Mineral Constraints on the Triassic Tectonic Evolution of the West Qinling Terrane, NW China: Implications for Understanding Subduction of the Paleotethyan Ocean

Author(s): Zhen Yan, Xianqing Guo, Changlei Fu, Jonathan Aitchison, Zongqi Wang, and Jiliang Li
Source: *The Journal of Geology*, Vol. 122, No. 5 (September 2014), pp. 591-608
Published by: The University of Chicago Press
Stable URL: http://www.jstor.org/stable/10.1086/677264
Accessed: 21/10/2015 21:24

Detrital Heavy Mineral Constraints on the Triassic Tectonic Evolution of the West Qinling Terrane, NW China: Implications for Understanding Subduction of the Paleotethyan Ocean

Zhen Yan,[1,2,] Xianqing Guo,[3] Changlei Fu,[1] Jonathan Aitchison,[2] Zongqi Wang,[3] and Jiliang Li[4]*

1. State Key Laboratory for Continental Tectonics and Dynamics, Institute of Geology, Chinese Academy of Geological Science, Beijing 100037, China; 2. School of Geosciences, University of Sydney, Sydney, New South Wales 2006, Australia; 3. Institute of Mineral Resources, Chinese Academy of Geological Science, Beijing 100037, China; 4. Institute of Geology and Geophysics, Chinese Academy of Science, Beijing 100029, China

ABSTRACT

We have examined the Triassic sediments in the west Qinling terrane, northeastern Tibet. These sediments consist mainly of flysch and shallow-sea and fluvial deposits with abundant lithic and heavy mineral detritus, sandwiched between and overlying Late Paleozoic and Early-Middle Triassic ophiolitic mélanges. Volcanic and metamorphic detritus dominates the lithic component of Lower Triassic sandstones accompanied by high Cr-spinel, pyroxene, and magnetite contents, indicating a mixed ophiolite and metamorphic source. Detrital mineral geochemistry further suggests that ophiolitic, high-grade metamorphic, basic, and intermediate-acidic igneous rocks must have been exposed and deeply eroded in their source area. Abundances of zircon, rutile, garnet, tourmaline, and epidote are greater in the Middle Triassic samples, and granitic and volcanic sources are the major contributors of detrital clasts. Considering these new observations on sedimentary petrography and detrital heavy mineral geochemistry, along with published data on paleocurrents, detrital zircon U-Pb ages, sedimentary facies, and regional magmatism, we suggest that these Triassic sediments represent the sedimentary fill of a forearc basin that overlies a late Paleozoic ophiolitic complex. A south-facing Andean-type convergent continental margin system developed along the southern margin of the North China block during the Triassic, in response to northward subduction of the Paleotethyan Ocean.

Online enhancements: appendix, supplementary tables.

Introduction

The west Qinling orogenic belt along the northeastern margin of the Tibet-Qinghai Plateau represents a geologically significant part of western China. It records the history of events within the Paleotethyan Ocean that once separated the North and South China cratons. Moreover, it is a transitional zone between the Qilian orogen to the northwest, the Kunlun orogen to the west, the Songpan-Ganzi terrane to the southwest, and other elements of the Qinling orogeny to the east.

Northward subduction of the Paleotethyan Ocean (Yan et al. 2008, 2012) during Triassic time generated a calc-alkaline margin arc system along the southern margin of North China. Detritus was shed from this continental margin to form sedimentary rocks in the west Qinling terrane (WQT). Although these Triassic sedimentary rocks are elsewhere regarded as an important ingredient of the Songpan-Ganzi Complex (Sengör 1987; Nie et al. 1994; Zhou and Graham 1996; Bruguier et al. 1997; Weislogel et al. 2010) or the west Qinling-Songpan continental tectonic node (Zhang et al. 2004), there is little agreement about the tectonic affinity of the WQT. Its provenance remains the subject of considerable debate and is mainly focused on the interpretation of detrital zircon U-Pb age spectra (Chen et al. 2009).

Provenance analysis of sedimentary basin depos-

Manuscript received August 19, 2013; accepted May 14, 2014; electronically published August 20, 2014.

* Author for correspondence; e-mail: yanzhen@mail.igcas.ac.cn.

[The Journal of Geology, 2014, volume 122, p. 591–608] © 2014 by The University of Chicago.
All rights reserved. 0022-1376/2014/12205-0006$15.00. DOI: 10.1086/677264

its is a widely applied tool in the reconstruction of the tectonic evolution of adjacent orogenic belts (Dickinson and Suczek 1979; Ingersoll et al. 1984; Dickinson 1985; Garzanti et al. 1996; Yan et al. 2006, 2008, 2012). Detrital heavy minerals are particularly useful for provenance analysis and paleotectonic reconstructions (Morton 1985, 1991; Garzanti et al. 1996; Cookenboo et al. 1997; Clift et al. 2012) because they are insensitive to modification during weathering, diagenesis, and sedimentation (Pettijohn 1941; Morton 1984). The unique chemical compositions of stable and ultrastable heavy minerals, such as garnet, tourmaline, apatite, spinel, chlorite, and zircon, are directly related to magma/fluid/protolith chemistry and metamorphism conditions. Certain unstable detrital minerals, such as pyroxenes and amphibole, can also be used to track arc evolution in convergent margin settings (Cawood 1991; Decou et al. 2011).

In order to contribute to this debate, we analyze the provenance of Triassic sandstones from the WQT, focusing on the chemical composition of detrital garnets, pyroxenes, amphiboles, and Cr-spinels. We discuss the implications of these new data in the context of the likely tectonic setting of these rocks in combination with petrology and published geochemistry and detrital zircon U-Pb data so as to refine understanding of the Triassic tectonic evolution of this important zone between the North and South China cratons where the extensive Paleotethyan Ocean once existed.

Geological Setting

The WQT is located along the northeastern margin of the Tibet-Qinghai Plateau (fig. 1). The Early Paleozoic Kunlun orogenic belt lies to the west across the Wahongshan fault, and other elements of the Qinling orogenic belt lie to the east. Northern and southern boundaries with the Early Paleozoic Qilian and Mesozoic Songpan-Ganzi orogenic belts are delineated by the Qinghai Lake fault (QHLF) and the A'nyemaqen fault (ANMQF), respectively. Abundant mafic-ultramafic rocks, pillow lava, gabbro, and radiolarian chert blocks crop out discontinuously and are locally overlain by Triassic sedimentary rocks of the WQT.

Early-Middle Triassic ophiolitic mélange along the ANMQF extends to the east and connects with the Mianlue ophiolitic mélange, representing the northeasternmost branch of the Paleotethyan Ocean (Lai et al. 2004). This belt separates the Paleozoic-Triassic subduction-accretion orogen to the north from Mesozoic collision-related thrust-fold belt to the south. The WQT is sandwiched between the Carboniferous-Permian ophiolitic mélange to the north and Early-Middle Triassic ophiolitic mélange to the south, connecting with the Triassic Andean-type magmatic arc belts of Kunlun orogenic belt in the west. It is generally considered to be an important part of the Songpan-Ganzi Complex because of the wide distribution of Triassic sediments.

Along the northern margin of the terrane, Carboniferous ophiolitic blocks, together with Proterozoic metamorphic and Silurian volcanic blocks, are tectonically intermingled in a Permian flysch-matrix mélange along the QHLF (Wang et al. 2000; BMGQ 2001; Guo et al. 2007). To the south, Cambrian-Ordovician and Carboniferous–early Permian ophiolitic blocks are tectonically intermingled within a Triassic flysch-matrix mélange along the ANMQF (Jiang et al. 1992; Xu et al. 1996; Bian et al. 2004; Yang et al. 2004; Zhang et al. 2004; Guo et al. 2007; Liu et al. 2011).

Along the boundary of the WQT with other elements of the Qinling terrane to the east, in the Tongren and Hezuo areas, mafic-ultramafic rocks, pillow lava, and gabbro blocks with oceanic island basalt (OIB) geochemical affinities and early-middle Permian limestone reef blocks lie within Lower to Middle Permian flysch matrix-mélange (Zhang et al. 2007; Wang et al. 2009). Further southeast in the Tanchang area (BMGG 1971), Devonian, Carboniferous, and Permian carbonate blocks are also mingled with ultramafic blocks and Permian flysch, in a zone that has been interpreted as a late Permian–early Triassic ophiolitic mélange (Li et al. 1978).

In the Saishitang and Gonghe areas of the west of the WQT, assemblages of Devonian-Permian mafic-ultramafic rocks, pillow lavas, gabbros, and radiolarian cherts are intermingled with Carboniferous-Permian carbonates, arc-related volcanic rocks and granitoids, and Proterozoic metavolcanic blocks (Wang et al. 2000; Sun et al. 2004). Pillow lavas in the Saishitang area exhibit typical enriched mid-ocean ridge basalt (MORB) geochemistry (Wang et al. 2000; Guo et al. 2007), possibly indicating origins in a back-arc basin related to a northward subduction of the Paleotethys (Yang et al. 2004).

Regionally, the ophiolitic mélanges are intruded by Triassic arc granites (Xiao et al. 2002; Jiang et al. 2010; Guo et al. 2012; Yan et al. 2012). Andesite, dacite, and rhyolite interlayers are common among the Middle Triassic sediments, and the Upper Triassic is dominated by andesites, indicating Middle to Late Triassic arc volcanism. The relative ages of

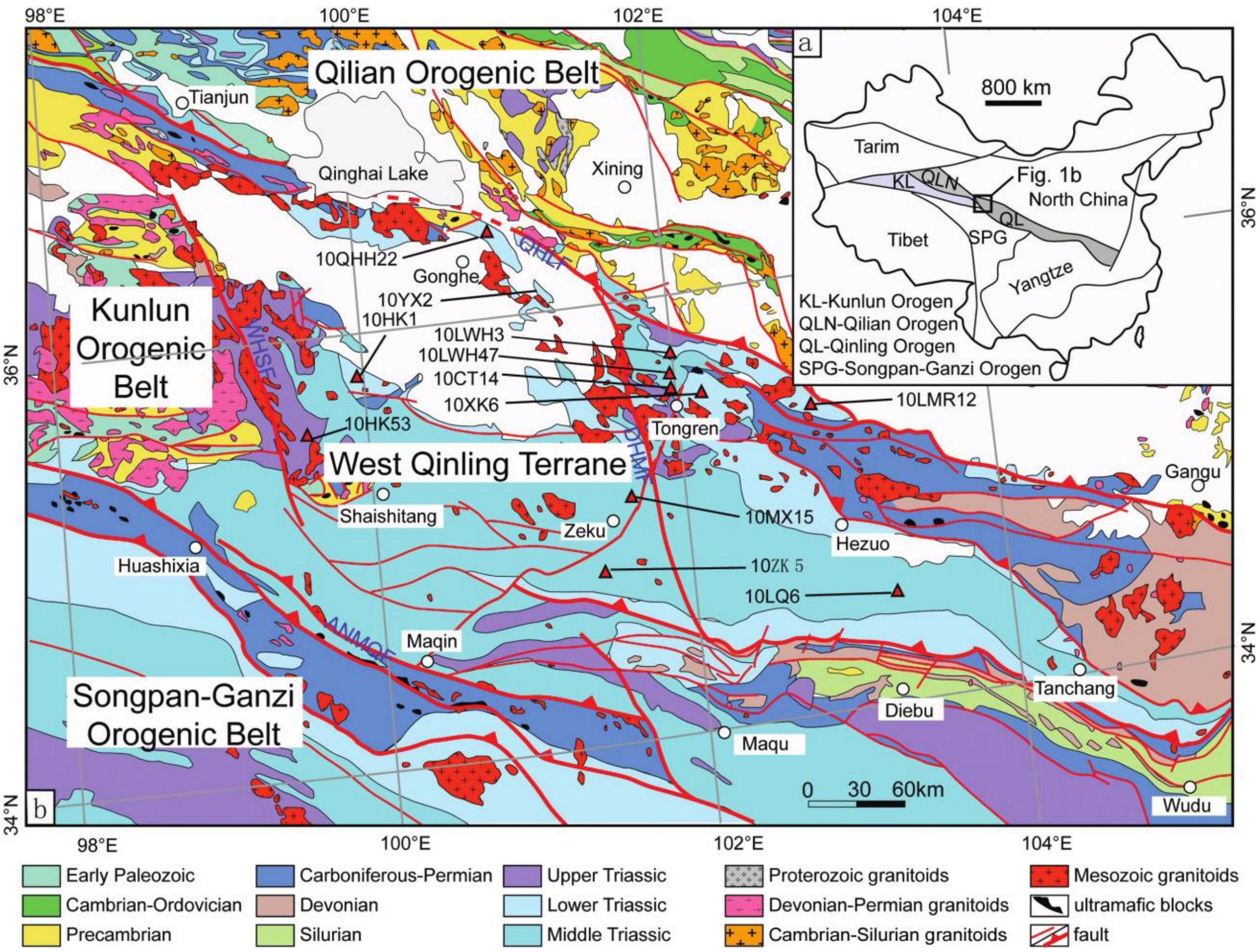

Figure 1. *a*, Location of the west Qinling terrane (WQT) within the tectonic framework of Chinese central orogenic belt, which is composed of the Qilian, Kunlun, and Qinling orogens. *b*, Regional geological map of the WQT showing the relationship between the Qilian, Kun, Qinling, and Songpan-Ganzi orogenic belts. QHLF = Qinghai Lake fault; ANMQF = A'nyemaqen fault; WHSF = Wahongshan fault; DHMF = Duohemao fault.

ophiolitic mélanges and accreted arc-related volcanic and granitoid rocks appear to progressively young southward across the WQT, implying southward trench migration during the evolution of the Paleotethys (Yan et al. 2012).

Triassic sedimentary-volcanic assemblages in the WQT have been subdivided into three regional-scale mappable units (BGMRGP 1989; BGMRQP 1991). The Lower Triassic Longwuhe Group consists of locally fossiliferous deep marine turbidite sediments typical of a submarine fan depositional setting (fig. 2). The Middle Triassic Gulangdi Formation mainly consists of sandstones and muddy siltstones locally with lenticular limestones and conglomerate interlayers. Abundant fossils indicate Middle Triassic deposition (BGMRGP 1989). The formation represents a large-scale sedimentary succession shallowing upward from proximal continental slope turbidites through to fluviodeltaic sediments in higher parts of the section. This likely reflects a significant event in the WQT. The Elashan Group is dominated by Late Triassic andesite, dacite, rhyolite, and pyroclastic rocks. It mainly crops out in the Tongren and west of Saishitang areas and exhibits Andean-style petrological characteristics. Together these rocks represent the products of convergent continental margin slope sedimentation from the Early to Middle Triassic.

Regionally, WQT Triassic sediments have been correlated with the Liufengguan Group in the Qinling orogen to the east and the Hongshuichuan and Naocangjian Formations in the Kunlun orogen to the west (BGMRGP 1989; BGMRQP 1991). They are also considered by some workers to be part of

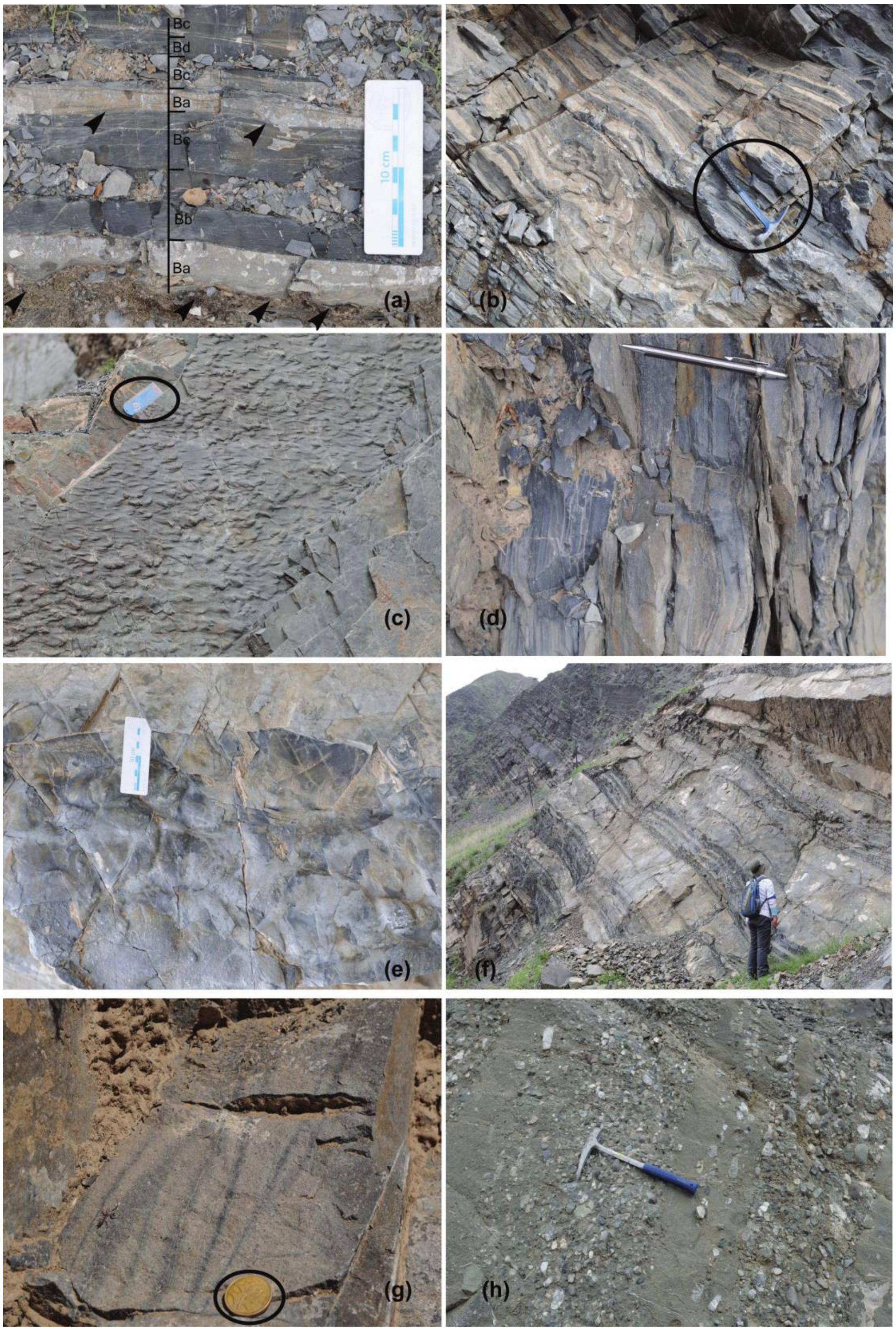
Bc
Bd
Bc
Ba
Bc
Bb
Ba
10 cm
(a)
(b)
(c)
(d)
(e)
(f)
(g)
(h)

the Sonpan-Ganzi terrane. However, few detailed studies exist, and correlations between terranes are not always straightforward. Numerous interpretations of the tectonic setting of WQT sediments have been proposed, including deposition in a strike-slip pull-apart basin (Feng et al. 2002; Sun et al. 2004), foreland basin (Zhang et al. 2004; Kou et al. 2007), rifted basin (Yin and Zhang 1998; Chen et al. 2009), relic oceanic basin (Yin and Nie 1993; Nie et al. 1994; Zhou and Graham 1996; Jiang et al. 1996), accretionary complex (Şengör 1985, 1987; Watson et al. 1987; Weislogel et al. 2010), or active continental margin (Jiang et al. 1996; Yan et al. 2008, 2012).

Sandstone Petrography

Sandstones of the Longwuhe Group are dominated by coarse-grained lithic arkose and litharenite containing abundant metamorphic and volcanic fragments. Those from the Gulangdi Formation consist mainly of feldspathic litharenite and lithic arkose, characterized by abundant feldspar and volcanic and granitic fragments with minor carbonate and metamorphic fragments (fig. 3).

Overall, the composition of sandstones is dominated by volcanic (average 26%), granitoid (average 38%), and metamorphic (average 28%) fragments, with minor (8%–20%) sedimentary fragments including chert, silty mudstone, and carbonate, indicating a continental arc source (Marsaglia and Ingersoll 1992). Both plagioclase (predominant) and alkali feldspar (minor) occur; however, mica is present within lithic arkoses. Quartz clasts range from 5% to 17% of framework grains, which is low in comparison to that of other grains. Most quartz grains are polycrystalline with obvious scaly inclusions and undulose extinction indicating metamorphic origins. Monocrystalline quartz shows undulatory extinction and contains common fluid inclusions that appear to be plutonic (Basu et al. 1975). Clear, fluid inclusion–free quartz with uniform extinction and embayment textures, interpreted to be volcanic in origin, is also common. Granitic and quartz fragments in some sandstone samples show distinct secondary corroded margins, probably as a result of diagenesis.

Compared with amphibole, pyroxene, and Cr-spinel, the detrital heavy mineral zircon, rutile, garnet, tourmaline, and epidote are very common in both the Lower and Middle Triassic sandstones from the WQT (fig. 4). Cr-spinel, pyroxene, and magnetite contents are higher in the Lower Triassic samples. With the exception of samples 10XK6 and 10LQ6, Cr-spinel, pyroxene, and amphibole contents are generally >1%. In contrast to Cr-spinel and pyroxene, relatively few amphibole grains were observed from only four of the sandstone samples. Garnet, zircon, and rutile are more abundant in Middle Triassic than Lower Triassic samples.

Sampling and Analytical Techniques

Twelve sandstone samples (>5 kg each) were collected from the Lower Triassic Longwuhe Group and the Middle Triassic Gulangdi Formation to study their detrital heavy mineral assemblage. Separation and preparation of heavy minerals followed standard procedures (Mange and Maurer 1992). About 352 grains were analyzed, with a total of 100 garnets, 90 clinopyroxenes, 118 Cr-spinels, and 44 amphiboles (see tables S1–S4, available online). The molecular end-members were calculated by the methods of Deer et al. (1997) and Morimoto (1988). In order to reflect the primary compositions of parent rocks, only data from the cores of the detrital Cr-spinels were used for calculations, and alteration rims were not measured in this study. Detrital pyroxene, amphibole, and garnet from the same sandstone samples were also used to complement provenance study for Cr-spinels. The detailed processes of separation and chemical component analysis and all analytical data are found in the appendix, available online.

Figure 2. Field photographs showing the characteristics of Triassic clastic rocks in the west Qinling terrane. Longwuhe Group: *a*, turbiditic sandstones and silty mudstone. Note distinct base erosion (arrowheads), normal grading (Ba), parallel (Bb, Bd), and ripple (Bc) laminations showing Bouma sequences. *b*, Slump folds of siltstone and mudstone. Hammer is 28 cm long. *c*, Sole marks at the base of turbiditic siltstone. Ruler is 10 cm long. Gulangdi Formation: *d*, turbiditic gray muddy sandstones (Babc) and deep-gray limestones (Bd). Pen is 14 cm long. *e*, Sole marks on turbiditic limestone. *f*, Lenticular, coarse-graded sandstone with trough bedding (see fig. 3*g*) and thin gray mudstone interlayers indicating a fluvial deposit. *g*, Trough cross stratification of coarse-graded sandstone. Coin is 2 cm in diameter. *h*, Lenticular conglomerate and coarse-graded sandstone interbeds with imbricative pebbles and trough cross stratification indicating an alluvial fan deposit. Hammer is 40 cm long.

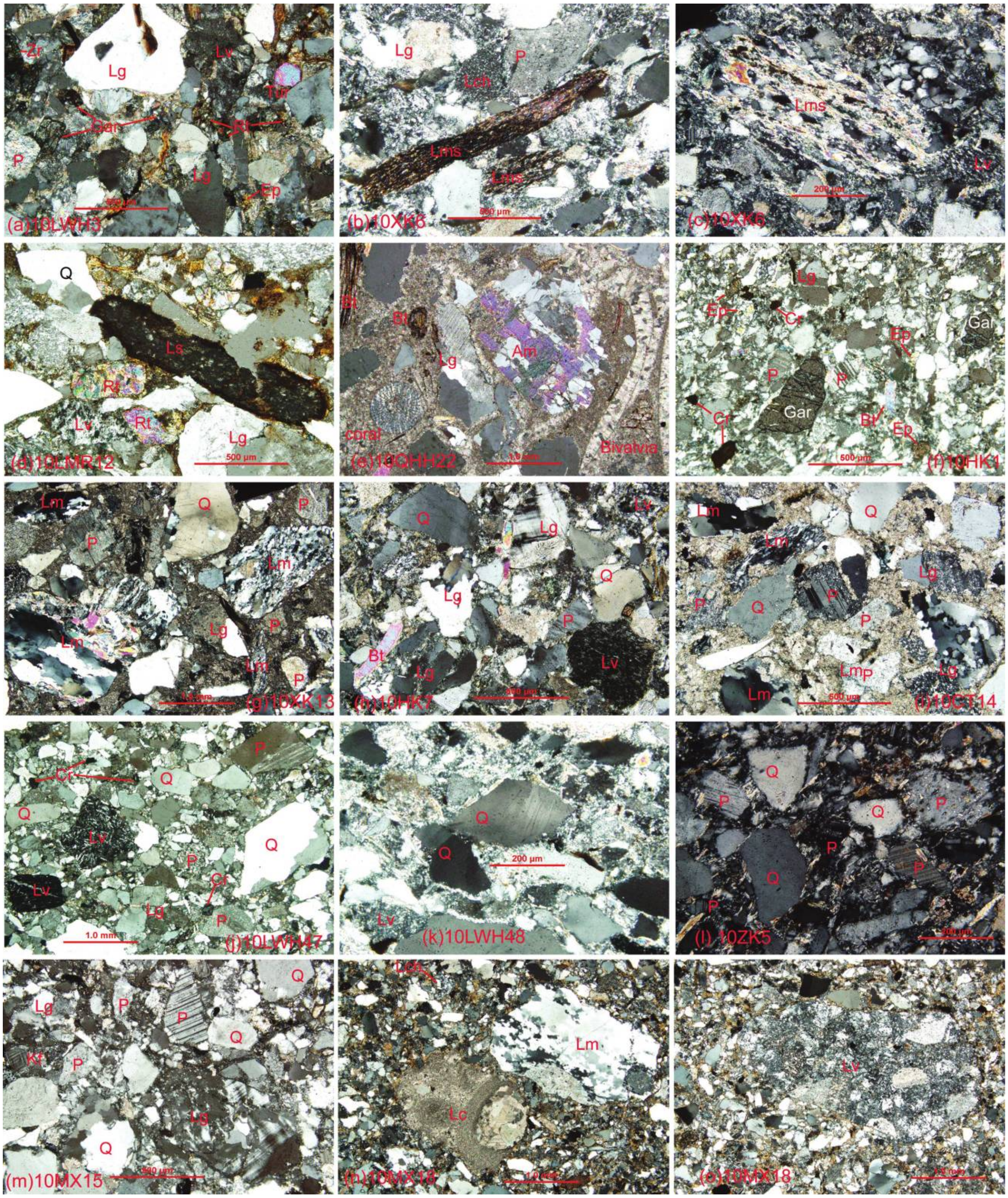

Figure 3. Photomicrographs of Triassic sandstone samples from the west Qinling terrane. *a–h*, *i–o*, Lower Triassic Longwuhe Group and Middle Triassic Gulangdi Formation, respectively. Lv = volcanic fragment; Lg = granitoid fragment; Lms = metamorphic fragment consisting of quartz and mica; Lm = granitoid gneiss fragment; Lch = chert fragment; Ls = silty mudstone fragment; Lc = carbonate fragment; P = plagioclase fragment; Kf = K-feldspar fragment; Q = quartz fragment; Ep = epidote; Rt = rutile; Gar = garnet; Bt = biotite; Cr = chrome spinel; Am =

Detrital Mineral Geochemistry

Cr-spinel grains are mostly subangular to rounded, elongated grains, typically 60–130 μm in length and 30–60 μm wide. They are brown to dark reddish-brown. Except for several grains with thin light margins and black cores, most are homogenous under scanning electron micrograph–backscattered electron analysis. Several grains from sample 10LWH3 exhibit distinct patchy textures. Large grains, >200 μm in diameter, are also nearly black with angular shapes. Some grain margins show conchoidal fractures, suggesting mechanical breakage, whereas other grains are subhedral-euhedral and preserve the original crystal boundary. The occurrence of euhedral crystals suggests that original chemical zonation produced during crystallization from the parental magma may be preserved in these grains. Several grains contain biotite and/or olivine inclusions.

Spinels from all seven samples show significant variations in important compositional parameters such as TiO_2, FeO/Fe_2O_3, $Mg/(Mg+Fe^{2+})$, and $Cr/(Cr+Al)$ (table 1). The Al_2O_3 contents of spinels from Middle Triassic samples (5.70–36.64 wt%) are higher than those from Lower Triassic samples (1.71–28.35 wt%), but their FeO^T contents are the reverse. The Cr_2O_3 content ranges from 14.89 to 61.4 wt% and is negatively correlated with Al_2O_3 content, which is in the range of 1.71–36.63 wt%. The maximum TiO_2 content is 1.13 wt% for the Middle Triassic sample. According to TiO_2 contents, those grains can be classified into high-Ti and low-Ti groups. The high-Ti group has less $Mg/(Mg+Fe^{2+})$ (=Mg#) than the low-Ti group in the same Cr#. The former mainly occur in the Middle Triassic samples, but the later mainly occur in the Lower Triassic samples. The Fe^{3+}# (atomic ratio $Fe^{3+}/(Cr+Al+Fe^{3+})$) varies from 0.01 to 1.21, and the Fe^{2+}/Fe^{3+} ratios are high (3–32). The Cr# and Mg# show a rough positive correlation, and the Cr# of most analyzed grains is higher than 50, which belongs to chromite and boninitic-type chromite.

Garnet is the most abundant heavy mineral species, especially in the Lower Triassic sandstone samples. They are predominantly represented by irregular, subangular, and subrounded crystals, and few grains are angular and rounded. Some grains show shallow corrosion-induced etch pits, and several grains have a thin dissolution margin composed of chlorite. Most are free from inclusions and colorless, but some display an orange or pale red color under plane-polarized light. Angular grains contain abundant quartz inclusions, with minor pyrite and K-feldspar inclusions. Quartz and ilmenite inclusions were also identified from several rounded grains.

All analyzed garnets usually have homogeneous compositions and do not show conspicuous chemical zoning. Strong compositional similarities exist between the detrital garnets from six sandstone samples in the WQT, although some minor differences are also present. Calculation of end-member garnet compositions revealed that the analyzed detrital garnets are rich in almandine component. Garnets from Lower Triassic samples are dominated by almandine with high pyrope and spessartine contents, but pyrope- and grossular-rich almandine mainly exist in the Middle Triassic samples. A lesser amount of almandine garnets have a high grossular content of 31.81%–38.81%, and three grains from a Middle Triassic sample have a high spessartine content of 43.71%–50.07%. Most almandine garnets have uvarovite content less than 1%.

Pyroxene is abundant, and almost all grains are angular to subangular, colorless to green black. Compositions range from Lower Triassic samples that are dominated by hedenbergite and diopside, with minor augite, pigeonite, and clinoferrosite to diopside and augite that dominate Middle Triassic

amphibole. *a*, Litharenite with abundant detrital heavy minerals (sample 10LWH3). *b*, Granitic, chert, and metamorphic siltstone fragments and plagioclase fragment in lithic arkose (sample 10XK6). *c*, Metamorphic sandstone fragment in lithic arkose (sample 10XK6). *d*, Silty mudstone, granitic and volcanic fragments, and rutile in litharenite (sample 10LMR2). *e*, Biotite, amphibole, coral, and bivalve fragments in lithic arkose (sample 10QHH22). *f*, Lithic arkose containing abundant detrital garnet, epidote, and chrome spinel. *g*, Abundant granitic gneiss fragments (Lm) and minor subangular quartz (Q) fragments in lithic arkose (sample 10XK13). Quartz fragment showing scaly inclusions and undulatory extinction. *h*, Volcanic and granitic fragments in litharenite (sample 10HK7). *i*, Lithic arkose with abundant metamorphic fragments. *j*, Angular volcanic and granitic fragments and detrital chrome spinel. *k*, Angular quartz fragments with scaly inclusions and undulatory extinction in litharenite (sample 10LWH48). *l*, Angular plagioclase and minor quartz fragments in lithic arkose (sample 10ZK5). *m*, Angular plagioclase and minor K-feldspar fragments and minor subangular quartz fragments with a secondary margin of lithic arkose (sample 10MX15). Granitic fragment shows typical granitic texture consisting of plagioclase and quartz (Lg). *n*, Carbonate (Lc) and gneiss (Lm) fragments and (0) volcanic fragments in litharenite (sample 10MX18).

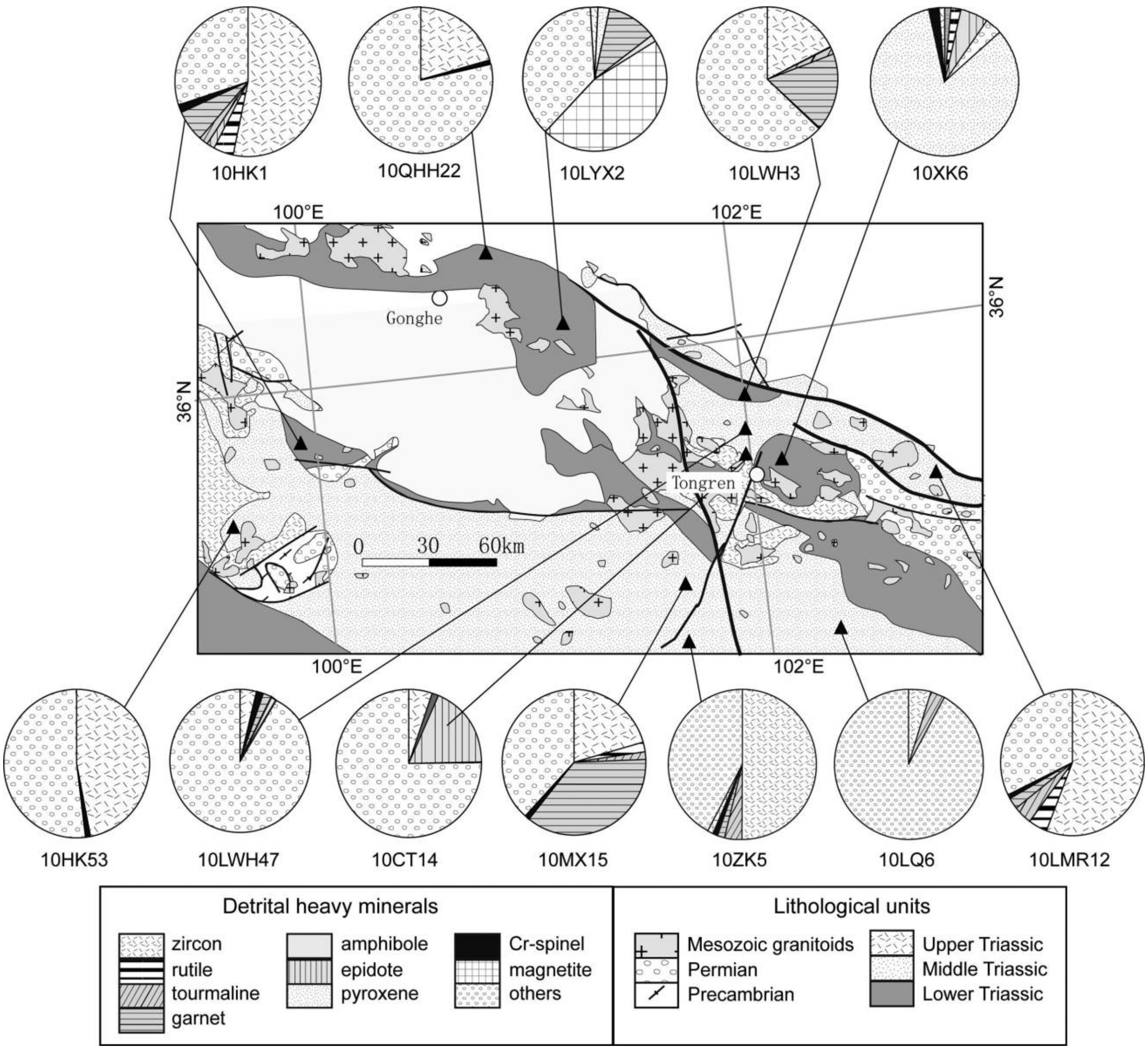

Figure 4. Pie charts showing compositional distribution of heavy mineral assemblages from the Lower and Middle Triassic sandstone samples of the west Qinling terrane.

samples. These grains have variable Al_2O_3 and SiO_2 contents and mainly plot within the nonalkaline field of Le Bas (1962).

Amphibole grains from four sandstone samples are angular to subangular and brown in color. They have variable SiO_2 contents (41.99–51.18 wt%), MgO (6.71–16.05 wt%), total FeO (12.31–24.93 wt%), Al_2O_3 (5.27–12.27 wt%), CaO (6.98–12.11 wt%), and low TiO_2 contents (0.09–2.65 wt%), MnO (0.08–0.66 wt%), Na_2O (0.55–1.59 wt%), K_2O (0.05–1.52 wt%), and very low Cr_2O_3 (<0.12 wt%). The low Na_2O+K_2O contents (0.76–2.8 wt%) are negatively related to their high Mg/(Mg+Fe), except for two grains with very low Na_2O+K_2O content. All analyzed amphiboles are Mg-rich (Mg/(Mg+Fe^{2+}) >0.5) calcic amphiboles according to the classification scheme of Leake (1978), which further divides into magnesiohornblende and pargasitic hornblende depending on whether Na+K in the A site is higher or lower than 0.5 atom formula (pfu).

Interpretation and Significance of Results

Lower and Middle Triassic sandstones in the WQT are dominated by poorly to moderately sorted feldspathic litharenite, lithic arkose, and litharenite with abundant lithic fragments, indicating depo-

Table 1. Al_2O_3 (wt%), TiO_2 (wt%), Cr_2O_3 (wt%), FeO^T (wt%), FeO/Fe_2O_3, $Mg/(Mg+Fe^{2+})$, and $Cr/(Cr+Al)$ of Detrital Cr-Spinels of the Triassic Clastic Rocks in the West Qinling Terrane

Strata	TiO_2	Al_2O_3	Cr_2O_3	FeO^T	FeO/Fe_2O_3	Mg#	Cr#	Fe^{3+}#
T_2	.2–1.13	5.95–29.97	24.14–61.4	16.62–40.50	1.32–18.57	.02–.72	.35–.87	.05–.42
T_2	0–.19	5.70–36.64	32.1–60.6	8.68–46.62	1.99–32.69	.03–.92	.37–1.00	.01–.51
T_1	0–.18	1.71–28.35	14.89–59.54	15.47–79.55	1.43–63.33	.06–.71	.49–.87	.01–1.21
T_1	.21–.53	5.55–23.11	39.64–60.09	20.23–45.79	2.33–6.41	.02–.61	.54–.85	.13–.45

sition on an active margin setting (Dickinson and Suczek 1979; Dickinson 1985; Marsaglia and Ingersoll 1992). Lithic clasts suggest that metamorphic, volcanic, and sedimentary rocks are exposed in source area, similar to the results of heavy mineral assemblage analyses. An increased abundance of metamorphic and sedimentary clasts together with detrital garnet, zircon, and rutile assemblage in the Middle Triassic sandstones indicate a significant metamorphic and sedimentary source, whereas basic volcanic rocks and ophiolites are the dominant source for the Lower Triassic sedimentary rocks. This is indicated through the greater abundance of volcanic clasts together with detrital amphibole, pyroxene, and Cr-spinels. Moreover, anomalously high concentrations of Cr, Ni, and V in the Triassic siltstones from the WQT (Yan et al. 2012; Zhang et al. 2012) also suggest an ophiolitic origin.

Cr-spinels are widely regarded as valid indicators of the petrogenetic history of mafic to ultramafic rocks, and their chemical composition is known to be influenced by the geotectonic environment in which they form (Irvine 1967; Evans and Frost 1975; Arai 1992; Barnes and Roeder 2001). The presence of detrital Cr-spinels in sedimentary rocks is generally regarded as important evidence of an ophiolitic source (Pober and Faupl 1988; Cookenboo et al. 1997; Hisada et al. 1999; Zhu et al. 2004).

According to Kamenetsky et al. (2001), TiO_2 and Al_2O_3 contents are negatively correlated in Cr-spinels from MORB, but those with arc origins do not show such correlation (fig. 5). All spinels show a large spread within the same discrimination field due to differences in Al_2O_3, and therefore they could be derived from island arc basalts, similar to the inference from their Cr# versus TiO_2 diagram (Pe-Piper et al. 2009). Those spinel grains within the low-Ti arc field likely originated from boninites and tholeiites with a suprasubduction zone (SSZ) affinity, but others within the high-Ti arc field are derived from calc-alkaline and high-K basalts (Kamenetsky et al. 2001). Some low-Ti spinels with a wide range of Cr# plot in the overlapping field between MORB and SSZ peridotite, indicating a forearc SSZ peridotite origin. Furthermore, the analyzed spinel grains predominately plot within the ophiolite field on the Fe^{3+}-Cr-Al diagram.

The high-Ti (>0.2 wt%) and low-Ti (<0.2 wt%) spinels have a high Cr# (40–87) and variable Al_2O_3 content (0.69–36.64 wt%), probably indicating a mixed host rock of SSZ harzburgites and back-arc basalts (Lenaz et al. 2000). Higher Fe^{3+}# contents of high-Ti spinels also suggest derivation from back-arc basalts (Arai 1992). Minor biotite inclusions probably indicate that those Cr-spinels should originate from a crustal contaminated magma. Thus, we suggest an interpretation of the host rock as originating in a subduction-related tectonic setting rather than MORB for the host rocks of most detrital spinels in the Lower and Middle Triassic sandstones.

Chemical data show that detrital Cr-spinels can be divided into high- and low-Ti groups, mainly in the Middle and Lower Triassic sandstones, respectively. The low-Ti group has a wide range of Cr#, but the high-Ti group also has a higher Fe^{3+}# content, with corresponding source rocks of forearc mantle wedge peridotites and back-arc basalts (Arai 1992; Hisada and Arai 1993) that were seriously eroded during the Early and Middle Triassic. Although no geochemical data for Cr-spinels are available, potential ophiolitic source rocks in the region occur along the QHLF (Wang et al. 2000). They were emplaced in the Tongren, Hezuo, and Shaishitang areas during the Devonian to Late Permian within/between the back-arc, forearc complex, and mid-ocean ridge environments within the broad suture zone (Li et al. 1978; Sun et al. 2004; Yang et al. 2004; Guo et al. 2007; Zhang et al. 2007; Wang et al. 2009). Furthermore, Cambrian-Ordovician ophiolite, the tectonic setting of which is disputed, and 455–440 Ma subduction-related mafic-ultramafic rocks (Yu et al. 2012; Zhang et al. 2012*a*, 2012*b*) in the Lajishan Mountains cannot be excluded as a potential source for the Cr-spinels. Paleocurrent data, heavy mineral assemblages, and detrital zircon U-Pb age spectra mitigate against derivation of Cr-spinel and pyroxene detritus from Early-Middle Triassic ophiolitic mélange along the ANMQF.

Garnets typically occur in a wide variety of meta-

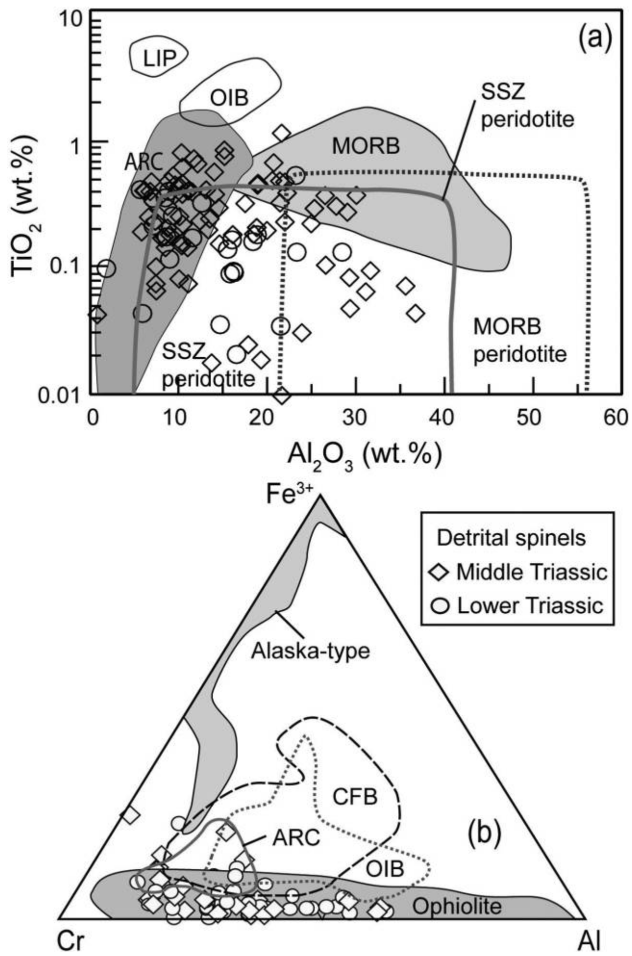

Figure 5. Geochemical discrimination diagrams for analyzed spinel grains. *a*, TiO_2 versus Al_2O_3 (wt%) diagram for Cr-spinels (after Kamenetsky et al. 2001). *b*, Fe^{3+} versus Cr versus Al ternary diagram (after Cookenboo et al. 1997). ARC = oceanic island arc; LIP = large igneous province; MORB = mid-ocean ridge basalt; OIB = oceanic island basalt; CFB = continental flood basalt; SSZ = suprasubduction zone.

morphic and igneous rocks, as well as in peraluminous rocks. According to the classification of Morton et al. (2004), detrital garnets from the Early and Middle Triassic sandstones are composed of type A, B, and C (fig. 6), which account for about 18%, 76%, and 6% of the analyzed garnet grains, respectively. Thus, they probably derived from amphibolite-facies metasedimentary rocks, granulite-facies metasedimentary rocks, and high-grade metabasic rocks. Moreover, some low-Ca and high-Mg garnets (type A) can also be derived from charnockites and intermediate-acidic igneous rocks (Sabeen et al. 2002; Morton et al. 2004). Type B grains are Mg- and Ca-poor but Mn-rich garnets that most likely originated from amphibolite-facies metasedimentary rocks (Deer et al. 1997). This suggests that amphibolite-facies metasedimentary rocks are the major source of detrital garnets in the Lower and Middle Triassic sandstones from the WQT and intermediate-acidic igneous and metabasic rocks are secondary source rocks. Quartz, chlorite, and K-feldspar inclusions probably also indicate a metamorphic origin.

Pyroxene composition is more rarely comprehensively studied in sedimentary rocks than are garnet and Cr-spinel, partly because of its unstable characteristics under weathering and diagenetic conditions. Studies of igneous rocks have shown that the great variations in chemical compositions of pyroxenes are directly related to the magma type and tectonic setting (Le Bas 1962; Nisbet and Pearce 1977; Leterrier et al. 1982). Thus, geochemistry of the detrital pyroxenes from sediments directly records changing magma compositions of their host rocks and provides further constraints to sediment provenance and to paleogeographic and plate tectonic reconstructions (Styles et al. 1989; Cawood 1991; Krawinkel et al. 1999; Pinto et al. 2007).

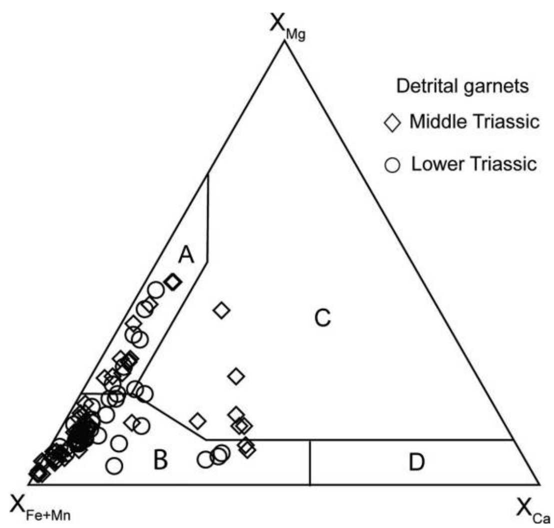

Figure 6. Ternary diagram of the end-member proportions of detrital garnet from the Lower and Middle Triassic sandstones of the west Qinling terrane. Fields A–D are after from Morton et al. (2004). Garnets in field A are mainly derived from high-grade granulite-facies metasediments or charnokites or minor intermediate-acidic igneous rocks. Garnets in field B are derived from amphibolite-facies metasediments. Garnets in field C are derived from high-grade metabasic rocks. Garnets in field D are generally derived from skarns and low-grade metabasic rocks or ultrahigh-temperature metamorphic calc-silicate granulites.

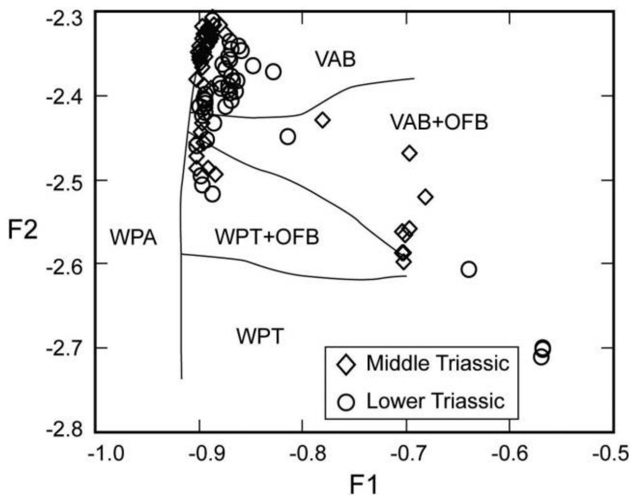

Figure 7. Plot of eigenvector-based discriminant functions F1 against F2 for detrital clinopyroxenes (after Nisbet and Pearce 1977). VAB = volcanic arc basalts; OFB = ocean floor basalts; WPT = within-plate tholeiitic basalts; WPA = within-plate alkali basalts.

Orogenic basalts, including island arc tholeiites, calc-alkaline, and shoshonitic basalts, are depleted in Cr and Ti with respect to the basalts from oceanic ridges, back-arc basins, continental rifts, and oceanic islands. The alkali basalts from oceanic and continental intraplate volcanism are enriched in Na and Ti and depleted in Si with respect to the other types of basalts. Clinopyroxenes from alkalic basalts are thus Al and Ti rich but Si poor with respect to clinopyroxenes from island arc tholeiites. The SiO_2 content of our samples ranges from 47.39 to 53.03 wt%, with corresponding Al_2O_3 and TiO_2 contents of 0.01–8.05 wt% and <0.9 wt%, respectively. About 85% of them show high Si (50–53 wt%) and low Al (<1 wt%) contents, indicating similarity to tholeiitic basalts. Although they are dominated by hedenbergite, diopside, and augite, nearly all of them plot within the subalkaline field on a SiO_2-Al_2O_3 covariation diagram (Le Bas 1962), consistent with erosion from a tholeiitic magmatic arc. Pyroxenes from Middle Triassic samples are similar to detrital pyroxenes from forearc sediments in both the Azeuro-Soná Complex of NW Panama (Krawinkel et al. 1999) and Murihiku terrane of New Zealand (Noda et al. 2004).

Samples mainly plot in field of volcanic island arc basalts and partially in field of oceanic-floor basalts (Nisbet and Pearce 1977) but lie close to the boundary of intraplate alkalic basalt (fig. 7). However, using the criteria of Leterrier et al. (1982), few grains in the Middle Triassic sandstones can be precisely related to nonorogenic basalts, and most are clearly related to alkalic basalts. Thus, we can infer that tholeiitic basalts with back-arc affinity are the most likely source of WQT detrital pyroxenes.

Hornblende in our samples is indicative of an intermediate to felsic calc-alkaline volcanic source (Deer et al. 1997). Decou et al. (2011) studied the chemistry of amphiboles from Cenozoic forearc sediments of the Central Andes and suggested that magnesio hornblende originated from volcanic arc rocks and amphibolites but pargasitic hornblende mainly originated from volcanic arc. In the FeO/MgO versus TiO_2/Al_2O_3 plot of Decou et al. (2011), our analyzed samples plot within the gneiss and amphibolites field, and half are close to the boundary of the volcanic arc field (fig. 8). This indicates that these amphiboles were derived from gneiss and amphibolites, some of which are components of the volcanic arc.

Possible Source Terranes

Regionally, the Hualong Complex, consisting of 500–400 and 940–850 Ma subduction-related calc-alkaline granitic and sedimentary rocks and >967 Ma high-grade metasedimentary rocks in the Lajishan Mountains (Z. Yan, unpublished data), is exposed along the northern margin of the WQT. The 496–445 and 246–238 Ma arc-related granites and 372–260 Ma collision-related granites widely occur in the west of the Hualong Complex (Wu et al. 2001; Qiang et al. 2007); 1.78–1.14 Ga granitic gneiss and older (>1.78 Ga) metasedimentary rocks also occur in SW Tianjun County and were interpreted as typical of basement rocks of the Olongbuluke terrane (Chen et al. 2007; Wang et al. 2008).

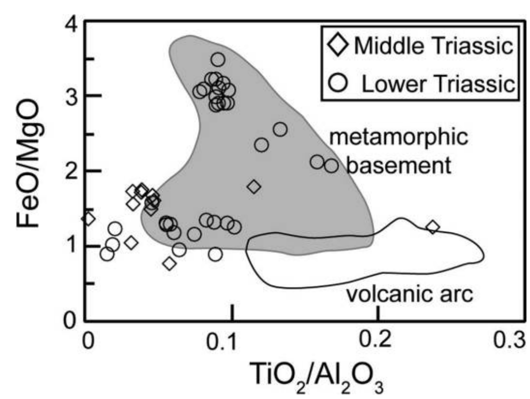

Figure 8. FeO/MgO versus TiO_2/Al_2O_3 covariation diagram of detrital amphiboles (fields after Decou et al. 2011).

The Hualong Complex provides a compatible source for the detrital mineral assemblage of garnets, amphiboles, rutile, epidote, and zircons present within Triassic WQT sandstones. Moreover, the age spectra for detrital zircon U-Pb ages from Triassic sandstones of the WQT indicate derivation from 300–250 Ma, 500–400 Ma, 1000–750 Ma, and 2.5–1.8 Ga rocks (Chen et al. 2009; Yan et al. 2012). On this basis, the Hualong Complex and 496–260 Ma granites in the northern margin of the WQT are interpreted as the most likely source.

Tectonic Setting. Several ophiolitic mélange belts with different ages ranging from Cambrian to Triassic are distributed around and within the WQT, indicating both long-lived and widespread subduction-accretion in the region. A Cambrian-Ordovician ophiolite and related subduction-accretionary complex in the Lajishan Mountains (Yan et al. 2012) were seriously modified by Silurian-Devonian accretion of a magmatic arc and an active continental margin formed during the Devonian along the northern margin of the WQT.

The presence of Devonian-Permian ophiolite along the QHLF (Li et al. 1978; Wang et al. 2000, 2009; Sun et al. 2004; Zhang et al. 2007) and synchronous arc magmatism (Wu et al. 2001; Qiang et al. 2007) along the northern margin of the WQT suggest the existence of a south-facing subduction system along the northern margin of the Paleotethys Ocean during the Permian. Precambrian blocks and Carboniferous limestone and OIB-type basalt blocks within Permian ophiolitic mélange in the Shaishitang area (Wang et al. 2000; Guo et al. 2007) may indicate that a Carboniferous seamount was accreted to the north during Permian subduction of the Paleotethys Ocean. Southward trench migration is suggested by formation of Early-Middle Triassic ophiolitic mélange that presently crops out in the Tongren area and along the ANMQF. Continental arc magmatism that developed widely along the south of the QHL (Gu et al. 1996; Qiang et al. 2007; Guo et al. 2012; Yan et al. 2012), together with arc magmatism in the Kunlun (Gu et al. 1996; Xiao et al. 2002) and Qinling (Jiang et al. 2010) mountains, indicates that an active continental margin could have developed along the northern margin of the Paleotethys Ocean during the Triassic. Thus, we interpret the Triassic sedimentary rocks in the WQT as forearc basin deposits developed on the flanks of this continental arc.

Discussion

Based mainly on regional comparison or detrital zircon dating, different interpretations have led to development of two main classes of thought regarding the geodynamic evolution of the WQT. One considers Triassic deposits to have formed in an active margin or forearc region in association with subduction-accretion of the Tethyan Ocean continuing during the Triassic (Şengör 1985, 1987; Yan et al. 2008, 2012; Weislogel et al. 2010). The other regards the Triassic deposits in the WQT as part of the Songpan-Ganzi terrane, where they formed in a relict ocean because of collision between the North China and the Yangtze plates during the Triassic (Yin and Nie 1993; Zhou and Graham 1996; Yin and Zhang 1998).

Weislogel (2008) and Weislogel et al. (2010) identified three depocenter zones (NE, NW, and east central) for the Songpan-Ganzi Complex based on regional variations in depositional facies, stratigraphy, and sediment composition. The WQT was considered the NE depocenter zone, with main sediment sources in the Qinling orogen and the North China block. It is separated from the east central depocenter zone by the Heishui fault (Weislogel 2008; Weislogel et al. 2010). Based on the petrology and geochemistry of sandstones, She et al. (2006) suggested the Kunlun and south Qinling orogens as major sediment contributors to the flysch in the NW and east central zones, respectively. Zhang et al. (2012) suggested that the Kunlun orogen was the main source area of the Triassic sediments near the west of the WQT, but the Qinling-Dabie orogen was the main contributor for Triassic flysch in the east of the WQT. Chen et al. (2009) suggested the Qilian-Kunlun orogen and Qaidam block as the contributors of the Triassic sediments in the WQT based on the detrital zircon U-Pb ages. However, Su et al. (2006), Lan et al. (2006), and Chen et al. (2006) suggested the Qinling orogen and the Yangtze block as the source area of Triassic flysch in the east central depocenter, which is different from the suggestion that it was the Yidun arc complex (Weislogel 2008; Weislogel et al. 2010) or Central Qiangtang ultrahigh-pressure belt (Zhang et al. 2012). Our results clearly demonstrate that the source area of the Triassic sediments in the WQT is distinctly different from that of sediment to the south of the ANMQF, indicating an alternative paleogeography during the Triassic.

Triassic sedimentary rocks in the WQT are dominated by deep- and shallow-sea and nonmarine deposits of the Middle Triassic Gulangdi Formation; however, coeval sediments south of the ANMQF are dominated by fluvial-lacustrine and tidal-flat deposits (Yan et al. 2008). Spatially, sedimentary rocks of the WQT are distributed between a Tri-

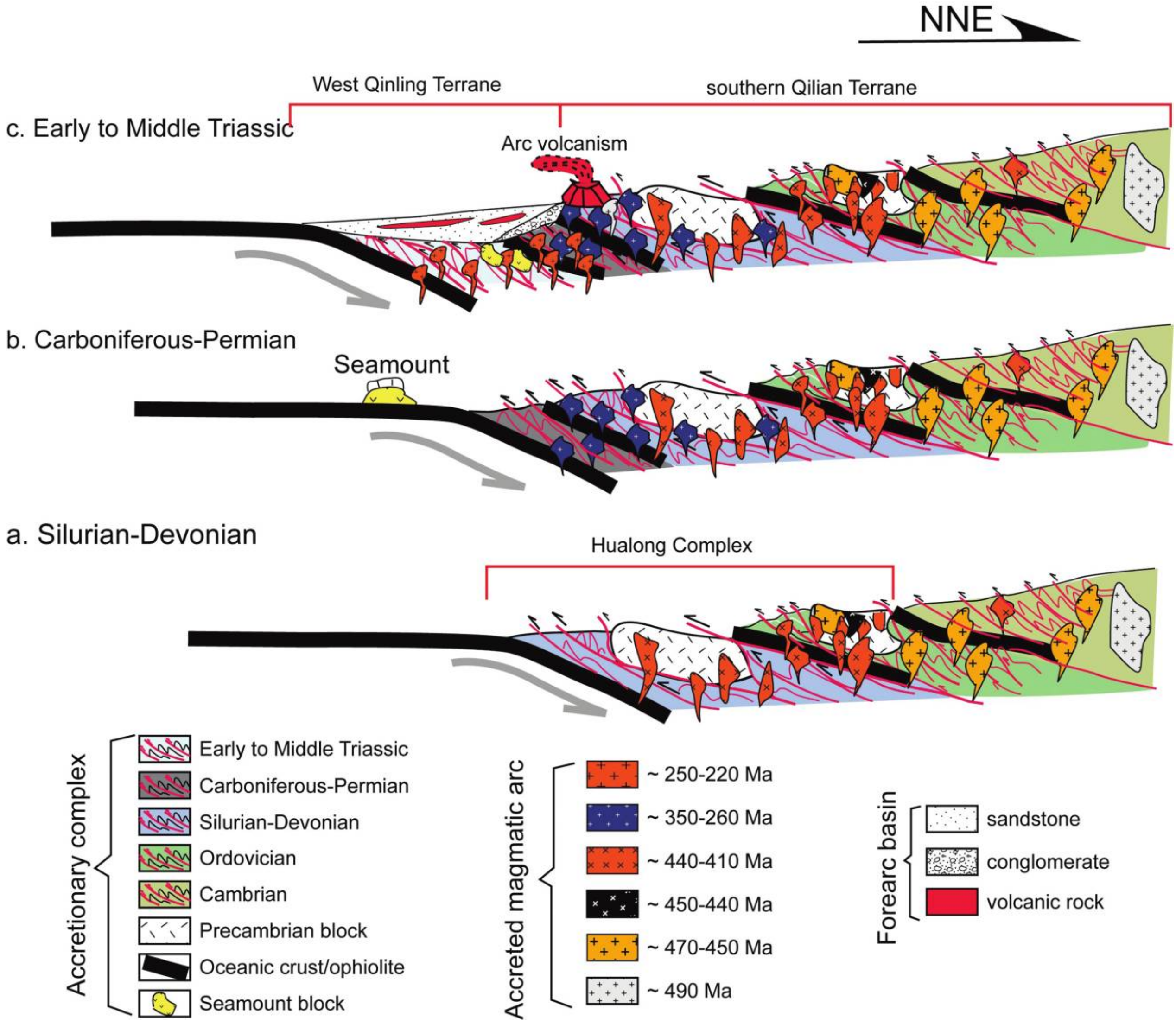

Figure 9. Cartoon illustrating a model for tectonic evolution of the northern margin of the Paleotethyan Ocean and west Qinling terrane.

assic Andean-type magmatic arc to the north (Gu et al. 1996; Jiang et al. 2010; Guo et al. 2012) and an Early-Middle Triassic ophiolitic mélange to the south (Jiang et al. 1992; Xu et al. 1996; Bian et al. 2004). A disrupted Late Paleozoic ophiolitic unit is overlapped by Lower and Middle Triassic sedimentary rocks.

Abundant Cr-spinel, pyroxene, and volcanic detritus together with anomalously high Cr and Ni concentrations in the siltstones (Yan et al. 2008, 2012) suggest that ophiolitic detritus is present in the Triassic deposits. Positive ε_{Nd} values and enrichment of ferromagnesian elements (Yan et al. 2012; Zhang et al. 2012) also point to significant contributions from ophiolitic fragments. Detrital Cr-spinel, pyroxenes, and amphibole geochemistries indicate a subduction-related source, evidently also indicating an arc or convergent margin settings for the Triassic deposits in the WQT (Cawood 1991; Decou et al. 2011). Furthermore, siltstone geochemistry and detrital modes both suggest deposition along an active continental margin (Yan et al. 2008, 2012; Chen et al. 2009).

Paleocurrent data suggest that the main source rocks for these Triassic sediments lie in the Qilian orogenic belt to the north of the WQT (Zhou and Graham 1996; Yan et al. 2008, 2012; Weislogel et al. 2010). This can also be inferred by a southward decrease in the abundance of detrital heavy minerals. Moreover, the textural maturity of angular to subangular detrital minerals and lithic fragments also suggests that they are source proximal.

Geochemistry and zircon Lu-Hf isotopic data for Early and Middle Triassic Andean-type granites in the WQT, Kunlun, and Qinling orogens suggest that melting of the ophiolitic rocks provided some contribution to the subduction-related arc magmatism (Xiao et al. 2002; Zhang et al. 2006; Guo et al. 2012; Li et al. 2013). These characteristics suggest that the Late Paleozoic ophiolitic mélange should be an important unit of the basement of the Triassic sedimentary rock in the WQT and an Andean-type continental margin developed along the NE margin of the Paleotethys Ocean in the Triassic. Therefore, we suggest that Triassic sedimentary rocks in the WQT represent forearc basin fill that is closely related to northward subduction of the Paleotethys Ocean.

Based on the constraints mentioned above, a brief summary of the Triassic tectonomagmatic and sedimentary evolution of the WQT is given in figure 9. According to this geodynamic scenario, combining the paleocurrent, detrital heavy mineral chemistry, and detrital zircon U-Pb data, northward subduction of Paleotethyan oceanic lithosphere during the Late Triassic led to development of an active continental margin along the area that presently forms the NE margin of the Tibet-Qinghai Plateau. Thus, the WQT was markedly different from the Sonpan-Ganzi Complex during the Triassic.

ACKNOWLEDGMENTS

We are grateful to Z. Chen and L. Yan for mount making and use of the electron probe microanalyzer. Careful reviews by G. Pe-Piper and D. Rowley focused our thinking and resulted in an improved version of this article. This research was financially supported by the National Natural Science Foundation of China (41372207, 41190072, 41772178, 41272221), the Key Program of the Ministry of Land and Resources of China (1212010911033, 1212011120159), and the China Scholarship Council Scholarship Program.

REFERENCES CITED

Arai, S. 1992. Chemistry of chromian spinel in volcanic rocks as potential guide to magma chemistry. Mineral. Mag. 56:173–184.

Barnes, S. J., and Roeder, P. L. 2001. The range of spinel compositions in terrestrial mafic and ultramafic rocks. J. Petrol. 42:2279–2302.

Basu, A.; Young, S. W.; Suttner, L. J.; James, W. C.; and Mack, G. H. 1975. Re-evaluation of the use of undulatory extinction and polycrystallinity in detrital quartz for provenance interpretation. J. Sediment. Petrol. 46:873–882.

BGMRGP (Bureau of Geology and Mineral Resources of Gansu Province). 1989. Regional geology of Gansu Province. Geological Memoir 19. Beijing, Geological Publishing House.

BGMRQP (Bureau of Geology and Mineral Resources of Qinghai Province). 1991. Regional geology of Qinghai Province. Geological Memoir 21. Beijing, Geological Publishing House.

Bian, Q.; Li, D.; Pospelov, I. I.; Yin, L.; Li, H.; Zhao, D.; Chang, C.; et al. 2004. Age, geochemistry and tectonic setting of Buqingshan ophiolites, north Qinghai-Tibet Plateau, China. J. Asian Earth Sci. 23:577–596.

BMGG (1st Geological Team of Geological Bureau of Gansu Province). 1971. Geological map and report of Lintan area. Scale 1 : 200,000 (in Chinese). Gansu Province, Geological Bureau.

BMGQ (5th Geological Team of Geological Survey of Institute of Qinghai Province). 2001. Geological maps of the Naerzong, Gaojiegenhao, Chahanhe and Zhonggaba areas. Scale 1 : 50,000 (in Chinese). Quinghai Province, Geological Survey.

Bruguier, O.; Lancelot, J.; and Malavieille, J. 1997. U-Pb dating on single detrital zircon grains from the Triassic Songpan-Ganze flysch (central China): provenance and tectonic correlations. Earth Planet. Sci. Lett. 152: 217–231.

Cawood, P. A. 1991. Characterisation of intra-oceanic magmatic arc source terranes by provenance studies of derived sediments. N. Z. J. Geol. Geophys. 34:347–358.

Chen, N.; Wang, Q.; Chen, Q.; and Li, X. 2007. Components and metamorphism of the basement of the Qaidam and Olongbuluke micro-continental blocks and a tentative interpretation of paleocontinental evolution in NW-Central China. Earth Sci. Frontiers 14: 43–55.

Chen, Y.; Tang, J.; Liu, F.; Zhang, H.; Nie, L.; and Jiang, L. 2006. Elemental and Sm-Nd isotopic geochemistry of clastic sedimentary rocks in the Garzê-Songpan block and Longmen Mountains. Geol. China 33:109–118.

Chen, Y.; Zhou, J.; Pi, Q.; Wang, Z.; and Li, D. 2009. Zircon U-Pb dating and geochemistry of clastic sedimentary rocks in the Gonghe-Huashixia Area, Qinghai Province and their geological implications. Earth Sci. Front. 16:161–174.

Clift, P. D.; Wares, N. M.; Amato, J. M.; Pavlis, T. L.; Hole, M. J.; Worthman, C.; and Day, E. 2012. Evolving heavy mineral assemblages reveal changing exhumation and trench tectonics in the Mesozoic Chugach accretionary complex, south-central Alaska. Geol. Soc. Am. Bull. 124:989–1006.

Cookenboo, H. O.; Bustin, R. M.; and Wilks, K. R. 1997. Detrital chromian spinel compositions used to reconstruct the tectonic setting of provenance: implications for orogeny in the Canadian Cordillera. J. Sediment. Res. 67:116–123.

Decou, A.; von Eynatten, H.; Mamani, M.; Sempere, T.; and Wörner, G. 2011. Cenozoic forearc basin sediments in southern Peru (15–18°S): stratigraphic and heavy mineral constraints for Eocene to Miocene evolution of the Central Andes. Sediment. Geol. 237:55–72.

Deer, W. A.; Howie, R. A.; and Zussman, J. 1997. Rock-forming minerals. Vol. 1A. Orthosilicates. 2nd ed. London, Geological Society, 919 p.

Dickinson, W. R. 1985. Interpreting provenance relations from detrital modes of sandstones. *In* Zuffa, G., ed. Provenance of arenites. NATO Adv. Stud. Inst. Ser. 148:333–361.

Dickinson, W. R., and Suczek, C. R. 1979. Plate tectonics and sandstone composition. Geol. Soc. Am. Bull. 108: 669–684.

Evans, B. W., and Frost, B. R. 1975. Chrome-spinel in progressive metamorphism: a preliminary analysis. Geochim. Cosmochim. Acta 39:959–972.

Feng, Y.; Cao, X.; and Zhang, E. 2002. Orogenic belt of the western Qinling. Xi'an, Xi'an Cartography Publishing House.

Garzanti, E.; Critelli, S.; and Ingersoll, R. 1996. Paleogeographic and paleotectonic evolution of the Himalayan Range as reflected by detrital modes of Tertiary sandstones and modern sands (Indus transect, India and Pakistan). Geol. Soc. Am. Bull. 108:631–642.

Gu, F.; Wu, X.; and Jiang, C. 1996. Assemblages and tectonic environment of the Variscan-Indosinian granitoid in the eastern Kunlun. Qinghai Geol. 1:18–36.

Guo, A.; Zhang, G.; Sun, Y.; Zheng, J.; Liu, Y.; and Wang, J. 2007. Geochemistry and spatial distribution of OIB and MORB in A'nyemaqen ophiolite zone: evidence of Majixueshan ancient ridge-centered hotspot. Sci. China Ser. D 50:197–208.

Guo, X.; Yan, Z.; Wang, Z.; Wang, T.; Hou, K.; Fu, C.; and Li, J. 2012. Middle-Triassic arc magmatism along the northeastern margin of the Tibet: U-Pb and Lu-Hf zircon characterization of the Gangcha complex in the west Qinling terrane, central China. J. Geol. Soc. Lond. 169:327–336.

Hisada, K., and Arai, S. 1993. Detrital chrome spinels in the Cretaceous Sanchu sandstone, central Japan: indicator of serpentinite protrusion into a fore-arc region. Palaeogeogr. Palaeoclimatol. Palaeoecol. 105:95–109.

Hisada, K.; Arai, S.; and Lee, Y. I.; 1999. Tectonic implication of lower Cretaceous chromian spinel-bearing sandstones in Japan and Korea. Isl. Arc 8:336–348.

Ingersoll, R. V.; Bullard, T. F.; Ford, R. L.; Grimm, J. P.; Pickle, J. D.; and Sares, S. W. 1984. The effect of grain size on detrital modes: a test of the Gazzi-Dickinson point-counting method. J. Sediment. Petrol. 49:103–116.

Irvine, T. N. 1967. Chromium spinel as a petrogenetic indicator. II. Petrologic applications. Can. J. Earth Sci. 4:71–103.

Jiang, C.; Yang, J.; and Feng, B. 1992. Opening-closing Tectonics of Kunlun Mountains. Beijing, Geological Publishing House.

Jiang, X.; Pan, G.; Yan, Y.; and Li, Z. 1996. Triassic sedimentary framework and tecto-paleogeographic evolution of the junction of the Qinling, Qilian and Kunlun orogenic belts. Acta Geol. Sichuan 16:204–208.

Jiang, Y.; Jin, G.; Liao, S.; Zhou, Q.; and Zhao, P. 2010. Geochemical and Sr-Nd-Hf isotopic constraints on the origin of Late Triassic granitoids from the Qinling orogen, central China: implications for a continental arc to continent-continent collision. Lithos 117:183–197.

Kamenetsky, V. S.; Crawford, A. J.; and Meffre, S. 2001. Factors controlling chemistry of magmatic spinel: an empirical study of associated olivine, Cr-spinel and melt inclusions from primitive rocks. J. Petrol. 42: 655–671.

Kou, X.; Zhu, Y.; Zhang, K.; Shi, B.; and Luo, G. 2007. Discovery and geochemistry of upper Permian volcanic rocks in Tongren area, Qinghai province and their tectonic significance. J. China Univ. Geosci. 32: 45–50.

Krawinkel, H.; Wozazek, S.; Krawinkel, J.; and Hellmann, W. 1999. Heavy-mineral analysis and clinopyroxene geochemistry applied to provenance analysis of lithic sandstones from the Azuero-Soná Complex (NW Panama). Sediment. Geol. 124:149–168.

Lai, S.; Wang, G.; and Li, S. 2004. Ophiolites from the Mianlue Suture in the southern Qinling and their relationship with the eastern Paleotethys evolution. Acta Geol. Sin. 78:107–117.

Lan, Z.; Chen, Y.; Su, B.; Liu, F.; and Zhang, H. 2006. The origin of sandstones from the Songpan-Ganze Basin, Sichuan, China: evidence from SHRIMP U-Pb dating of clastic zircons. Acta Sedimentol. Sin. 24:321–332.

Leak, B. E. 1978. Nomenclature of amphiboles. Am. Mineral. 63:1023–1052.

Le Bas, M. J. 1962. The role of aluminium in igneous clinopyroxenes with relation to their parentage. Am. J. Sci. 260:267–288.

Lenaz, D.; Kamenetsky, V. S.; Crawford, A. J.; and Princivalle, F. 2000. Melt inclusions in detrital spinel from the SE Alps (Italy-Slovenia): a new approach to provenance studies of sedimentary basins. Contrib. Mineral Petrol. 139:748–758.

Leterrier, J.; Maury, R.; Thonon, P.; Girard, D.; and Marchal, M. 1982. Clinopyroxene composition as a method of identification of the magmatic affinities of paleo-volcanic series. Earth Planet. Sci. Lett. 59:139–154.

Li, C. Y.; Liu, Y. W.; and Zhu, B. Q. 1978. Tectonic evolution of Qinling and Qilian mountains. International Collected Geological Research Works. Beijing, Geological Publishing House, p. 174–187 (in Chinese).

Li, X.; Mo, X.; Yu, X.; Ding, Y.; Huang, X.; Wei, P.; and

He, W. 2013. Petrology and geochemistry of the early Mesozoic pyroxene andesites in the Maixiu Area, west Qinling, China: products of subduction or syn-collision? Lithos 172–173:158–174.

Liu, Z. Q.; Pei, X. Z.; Li, R. B.; Li, Z. C.; Zhang, X. F.; Liu, Z. G.; Chen, G. C.; Chen, Y. X.; Ding, S. P.; and Guo, J. F. 2011. LA-ICP-MS zircon U-Pb geochronology of the two suites of ophiolites at the Buqingshan area of the A'nyemaqen orogenic belt in the southern margin of east Kunlun and its tectonic implication. Acta Geol. Sin. 85:185–194.

Mange, M. A., and Maurer, H. F. W. 1992. Heavy minerals in colour. London, Chapman & Hall, 147 p.

Marsaglia, K. M., and Ingersoll, R. V. 1992. Compositional trends in arc-related, deep-marine sand and sandstone: a reassessment of magmatic-arc provenance. Geol. Soc. Am. Bull. 104:1637–1649.

Morimoto, N. 1988. Nomenclature of pyroxenes. Am. Mineral. 73:1123–1133.

Morton, A. C. 1984. Stability of detrital heavy minerals in Tertiary sandstones of the North Sea Basin. Clay Miner. 19:287–308.

———. 1985. A new approach to provenance studies: electron microprobe analysis of detrital garnets from Middle Jurassic sandstones of the northern North Sea. Sedimentology 32:553–566.

———. 1991. Geochemical studies of detrital heavy minerals and their application to provenance research. Geol. Soc. Lond. Spec. Publ. 57:31–45.

Morton, A. C.; Hallsworth, C. R.; and Chalton, B. 2004. Garnet compositions in Scottish and Norwegian basement terrains: a framework for interpretation of North Sea sandstone provenance. Mar. Petrol. Geol. 21:393–410.

Nie, S.; Yin, A.; Rowley, D. B.; and Jin, Y. 1994. Exhumation of the Dabie Shan ultrahigh-pressure rocks and accumulation of the Songpan-Ganzi flysch sequence, central China. Geology 22:999–1002.

Nisbet, E. G., and Pearce, J. A. 1977. Clinopyroxene compositions in mafic lavas from different tectonic settings. Contrib. Mineral. Petrol. 63:149–160.

Noda, A.; Takeuchi, M.; and Adachi, M. 2004. Provenance of the Murihiku terrane, New Zealand: evidence from the Jurassic conglomerates and sandstones in Southland. Sediment. Geol. 164:203–222.

Pe-Piper, G.; Tsikouras, B.; Piper, D. J. W.; and Triantaphyllidis, S. 2009. Chemical fingerprinting of detrital minerals in the Upper Jurassic-Lower Cretaceous sandstones, Scotian Basin. Geol. Surv. Can. Open-File Rep. 6288, 150 p.

Pettijohn, F. J. 1941. Persistence of heavy minerals and geologic age. J. Geol. 49:610–625.

Pinto, L.; Hérail, G.; Fontan, F.; and de Parseval, P. 2007. Neogene erosion and uplift of the western edge of the Andean Plateau as determined by detrital heavy mineral analysis. Sediment. Geol. 195:217–237.

Pober, E., and Faupl, P. 1988. The chemistry of detrital chromian spinels and its implications for the geodynamic evolution of the eastern Alps. Geol. Rundsch 77:641–670.

Qiang, J.; Guo, A.; and Sun, Y. 2007. Geochemistry of granitoids of the Zongwulongshan tectonic zone and geological significance. J. Northwest. Univ. 37:98–102.

Sabeen, H. M.; Ramanujam, N.; and Morton, A. C. 2002. The provenance of garnet: constraints provided by studies of coastal sediments from southern India. Sediment. Geol. 152:279–287.

Şengör, A. M. C. 1985. East Asia tectonic collage. Nature 318:16–17.

———. 1987. Tectonics of the Tethysides: orogenic collage development in a collisional setting. Annu. Rev. Earth Planet. Sci. 15:213–244.

She, Z.; Ma, C.; Masona, R.; Li, J.; Wang, G.; and Lei, Y. 2006. Provenance of the Triassic Songpan-Ganzi flysch, west China. Chem. Geol. 231:159–175.

Styles, M. T.; Stone, P.; and Floyd, J. D. 1989. Arc detritus on the southern Uplands: mineralogical characterization of a "missing terrane." J. Geol. Soc. 146:397–400.

Su, B.; Chen, Y.; Liu, F.; Wang, Q.; Zhang, H.; and Lan, Z. 2006. Geochemical characteristics and significance of Triassic sandstones of Songpan-Ganze block. Acta Petrol. Sin. 22:961–970.

Sun, Y.; Zhang, G.; Wang, J.; Zhan, F.; and Zhang, Z. 2004. $^{40}Ar/^{39}Ar$ age of the basic swarms of two periods in the junction area of Qinling and Kunlun and its tectonic significance. Acta Geol. Sin. 78:65–71.

Wang, B.; Zhang, Z.; Zhang, S.; Zhu, Y.; and Cao, S. 2000. Geological features of lower Paleozoic ophiolite in Kuhai-Saishitang region, eastern section of eastern Kunlun. J. China Univ. Geosci. 25:592–598.

Wang, H.; Zhu, Y.; Lin, Q.; and Li, Y. 2009. Mineral characteristics and tectonic environment of Longwuxia Gorge ophiolite in Tongren, west Qinling area. Acta Petrol. Mineral. 28:316–328.

Wang, Q.; Chen, N.; Li, X.; Hao, S.; and Chen, H. 2008. LA-ICPMS zircon U-Pb geochronological constraints on the tectonothermal evolution of the Early Paleoproterozoic Dakendaban Group in the Quanji Block, NW China. Chin. Sci. Bull. 53:2849–2858.

Watson, M. P.; Hayward, A. B.; Parkinson, D. N.; and Zhang, Z. M. 1987. Plate tectonic history, basin development and petroleum source rock deposition onshore China. Mar. Petrol. Geol. 4:205–225.

Weislogel, A. L. 2008. Tectonostratigraphic and geochronologic constraints on evolution of the northeast Paleotethys from the Songpan-Ganzi complex, central China. Tectonophysics 451:331–345.

Weislogel, A. L.; Graham, S. A.; Chang, E. Z.; Wooden, J. L.; and Gehrels, G. E. 2010. Tectonics, erosional exhumation, and sediment production Upper Triassic Songpan-Ganzi complex, central China: record of collisional detrital zircon provenance from three turbidite depocenters. Geol. Soc. Am. Bull. 122:2041–2062.

Wu, C.; Yang, J.; Ireland, T.; Wooden, J.; Li, H.; Wan, Y.; and Shi, R. 2001. Zircon SHRIMP ages of Aolaoshan granite from the south margin of Qilianshan and its geological significance. Acta Petrol. Sin. 17:215–221.

Xiao, W. J.; Windley, B. F.; Chen, H. L.; Zhang, G. C.; and

Li, J. L. 2002. Carboniferous-Triassic subduction and accretion in the western Kunlun, China: implications for the collisional and accretionary tectonics of the northern Tibetan Plateau. Geology 30:295–298.

Xu, Z. Q.; Yang, J. S.; and Chen, F. Y. 1996. The A'nyemaqen suture belt and the dynamics in subduction and collision. *In* Zhang, Q., ed. Study on ophiolites and geodynamics. Beijing, Geological Publishing House, p. 185–189 (in Chinese).

Yan, Z.; Bian, T.; Korchagin, O. A.; Pospelov, I. I.; Li, J.; and Wang, Z. 2008. Provenance of early Triassic Hongshuichuan Formation in the southern margin of the east Kunlun Mountains: constrain from detrital framework, heavy mineral analysis and geochemistry. Acta Petrol. Sin. 24:1068–1078.

Yan, Z.; Wang, Z.; Li, J.; Xu, Z.; and Deng, J. 2012. Tectonic settings and accretionary orogenesis of the west Qinling terrane, northeastern margin of the Tibet Plateau. Acta Petrol. Sin. 28:1808–1828.

Yan, Z.; Wang, Z.; Wang, T.; Yan, Q.; Xiao, W.; and Li, J. 2006. Provenance and tectonic setting of clastic deposits in the Devonian Xicheng basin, Qinling orogen, central China. J. Sediment. Res. 76:557–574.

Yang, J.; Wang, X.; Shi, R.; Xu, Z.; and Wu, C. 2004. The Dur'ngoi ophiolite in east Kunlun, northern Qinghai-Tibet Plateau: a fragment of paleo-Tethyan oceanic crust. Chin. Geol. 31:225–239.

Yin, A., and Nie, S. 1993. An indentation model for the North and South China collision and the development of the Tan-Lu and Honam fault systems, eastern Asia. Tectonics 12:801–813.

Yin, H. F., and Zhang, K. X. 1998. Evolution and characteristics of the central orogenic belt. J. China Univ. Geosci. 23:438–442.

Yu, J.; Li, X.; Ma, Z.; Wang, G.; Tang, Z.; Sun, J.; and Wu, P. 2012. Zircon U-Pb dating of the Yishichun mafic-ultramafic complex from southern Qilian and its geological significance. J. China Univ. 18:158–163.

Zhang, G.; Guo, A.; and Yao, P. 2004. Western Qinling-Songpan continental tectonic node in China's continental tectonics. Earth Sci. Front. 11:23–32.

Zhang, H.; Chen, Y.; Xu, W.; Liu, R.; Yuan, H.; and Liu, X. 2006. Granitoids around Gonghe basin in Qinghai Province: petrogenesis and tectonic implications. Acta Petrol. Sin. 22:2910–2922.

Zhang, K.; Li, B.; and Wei, Q. 2012. Diversified provenance of the Songpan-Ganzi Triassic turbidites, central China: constraints from geochemistry and Nd isotopes. J. Geol. 120:69–82.

Zhang, K.; Lin, Q.; Zhu, Y.; Yin, H.; Luo, M.; Chen, N.; and Wang, G. 2004. New paleontological evidence on time determination of the east part of the eastern Kunlun mélange and its tectonic significance. Sci. China Ser. D 47:865–873.

Zhang, K.; Zhuang, Y.; Lin, Q.; Kou, X.; Fan, G.; Chen, F.; and Luo, G. 2007. Discovery of a mafic-ultramafic belt in the Rongwoxia area, Tongren, Qinghai, China. Geol. Bull. China 28:63–71.

Zhang, Z.; Li, W.; Gao, Y.; Xie, X.; Wang, Y.; Zhang, J.; Guo, Z.; and Li, K. 2012*a*. Geochemical characteristics of the Lashuixia basic complex in Qinghai province on its constraints on genesis of the deposit. Geol. Explor. 48:959–968.

Zhang, Z.; Li, W.; Gao, Y.; Zhang, J.; Guo, Z.; and Li, K. 2012*b*. ID-TIMS zircon U-Pb age of Yulonggou intrusive rocks in southern Qilian Mountain and its geological significance. Geol. Bull. China 31:455–462.

Zhou, D., and Graham, S. A. 1996. Songpan-Ganzi Triassic flysch complex of the west Qinling Shan as a remnant ocean basin. *In* Yin, A., and Harrison, M., eds. The tectonic evolution of Asia. Cambridge, Cambridge University Press, p. 281–299.

Zhu, B.; Kidd, W. S. F.; Rowley, D.; and Currie, B. 2004. Chemical compositions and tectonic significance of chrome-rich spinels in the Tianba flysch, southern Tibet. J. Geol. 112:417–434.